ORIGINAL RESEARCH

Bagcilar Med Bull 2026;11(1):124-138
DOI: 10.4274/BMB.galenos.2026.95866

Quercetin Protects Against Doxorubicin-induced Cardiac Injury Through Stress Modulation: Evidence from Electrocardiographic, Scintigraphic, and Biochemical Analyses in Rats

Quercetin, Stres Modülasyonu Yoluyla Doksorubisin Kaynaklı Kalp Hasarına Karşı Koruma Sağlar: Sıçanlarda Elektrokardiyografik, Sintigrafik ve Biyokimyasal Analizlerden Elde Edilen Kanıtlar

Musa Salmanoğlu[1], Habip Yılmaz[2], Gülçin Ercan[3], Murat Kalın[3], Serdar Savaş Gül[4], Fadime Demir[5], Aylin Arslan[3], Hatice Aygün[6]

[1]University of Health Sciences Turkey, Sultan 2. Abdülhamid Han Training and Research Hospital, Department of Internal Medicine, İstanbul, Turkey
[2]University of Health Sciences Turkey, Sultan 2. Abdülhamid Han Training and Research Hospital, Department of Anesthesiology and Reanimation, İstanbul, Turkey
[3]University of Health Sciences Turkey, İstanbul Prof. Dr. Cemil Taşcıoğlu City Hospital, Department of General Surgery, İstanbul, Turkey
[4]Lokman Hekim University Faculty of Medicine, Department of Nuclear Medicine, Ankara, Turkey
[5]University of Health Sciences Turkey, Kayseri City Training and Research Hospital, Department of Nuclear Medicine, Kayseri, Turkey
[6]Biruni University, Neuroscience Laboratory, BAMER, İstanbul, Turkey

Abstract

Objective: Doxorubicin (DOX) induces cardiotoxicity via oxidative and endoplasmic reticulum (ER) stress. This study evaluated the cardioprotective effects of quercetin against DOX-induced cardiac injury in rats, focusing on ER stress and SIRT1 signaling.

Method: Wistar Albino rats were used. Rats were allocated into control, DOX, low-dose quercetin (10 mg/kg) + DOX, and high-dose quercetin (100 mg/kg) + DOX groups. Cardiac function was assessed by lead II electrocardiography, while myocardial injury was evaluated using Tc-99m pyrophosphate (PYP) scintigraphy. Cardiac biomarkers, inflammatory cytokines, oxidative stress parameters, ER stress markers, and SIRT1 expression were analyzed.

Results: DOX induced marked electrocardiogram abnormalities, including Q wave-T wave interval- prolongation and ST-segment elevation, increased myocardial ^{99}mTc-PYP uptake, elevated cardiac injury biomarkers, renal and hepatic markers, enhanced

Öz

Amaç: Doksorubisin (DOX), oksidatif ve endoplazmik retikulum (ER) stresi yoluyla kardiyotoksisiteye neden olur. Bu çalışma, ER stresi ve SIRT1 sinyaline odaklanarak, sıçanlarda DOX'in neden olduğu kalp hasarına karşı quercetinin kardiyoprotektif etkilerini değerlendirmiştir.

Yöntem: Wistar Albino sıçanlar kullanılmıştır. Sıçanlar kontrol, DOX, düşük doz quercetin (10 mg/kg) + DOX ve yüksek doz quercetin (100 mg/kg) + DOX gruplarına ayrılmıştır. Kardiyak fonksiyon II elektrokardiyografi ile değerlendirilirken, miyokardiyal hasar Tc-99m pirofosfat (PYP) sintigrafisi kullanılarak değerlendirilmiştir. Kardiyak biyobelirteçler, enflamatuvar sitokinler, oksidatif stres parametreleri, ER stres belirteçleri ve SIRT1 ekspresyonu analiz edildi.

Bulgular: DOX, Q dalgası-T dalgası aralığı uzaması ve ST segment yükselmesi, miyokardiyal ^{99}mTc-PYP alımında artış, kardiyak hasar biyobelirteçlerinde, böbrek ve karaciğer belirteçlerinde yükselme,

Address for Correspondence: Hatice Aygün MD, Biruni University, Neuroscience Laboratory, BAMER, İstanbul, Turkey
E-mail: hatice_5aygun@hotmail.com **ORCID:** orcid.org/0000-0002-4272-0562
Received: 21.01.2026 **Accepted:** 12.03.2026 **Publication Date:** 18.03.2026

Cite this article as: Salmanoğlu M, Yılmaz H, Ercan G, Kalın M, Gül SS, Demir F, et al. Quercetin protects against doxorubicin-induced cardiac injury through stress modulation: evidence from electrocardiographic, scintigraphic, and biochemical analyses in rats. Bagcilar Med Bull. 2026;11(1):124-138

Abstract

oxidative stress, inflammatory responses (tumor necrosis factor-α, interleukin-6), upregulation of GRP78 and C/EBP homologous protein, and suppression of SIRT1 and glutathione ($p<0.05$). Quercetin significantly attenuated these alterations in a dose-dependent manner, with greater protection observed at the higher dose.

Conclusion: Quercetin mitigates DOX-induced cardiotoxicity by suppressing oxidative stress, ER stress, and inflammation via restoration of SIRT1 signaling. The integration of electrocardiography and Tc-99m PYP scintigraphy provides novel multimodal evidence of quercetin's cardioprotective effects.

Keywords: Cardiotoxicity, doxorubicin, ER stress, oxidative stress, quercetin, scintigraphy

Öz

oksidatif stres artışı, enflamatuvar yanıtlarda (tümör nekroz faktörü-α, interlökin-6) artış, GRP78 ve C/EBP homolog proteinin yukarı regülasyonu ve SIRT1 ve glutatyonun baskılanması ($p<0,05$) gibi belirgin elektrokardiyografi anormalliklerine neden olmuştur. Quercetin, bu değişiklikleri doz bağımlı bir şekilde önemli ölçüde azalttı ve daha yüksek dozda daha fazla koruma gözlendi.

Sonuç: Quercetin, SIRT1 sinyalini geri yükleyerek oksidatif stresi, ER stresini ve enflamasyonu baskılayarak DOX'in neden olduğu kardiyotoksisiteyi hafifletir. Elektrokardiyografi ve Tc-99m PYP sintigrafisinin entegrasyonu, quercetinin kardiyoprotektif etkilerine ilişkin yeni multimodal kanıtlar sağlar.

Anahtar kelimeler: Doksorubisin, ER stresi, kardiyotoksisite, oksidatif stres, quercetin, sintigrafi

Introduction

Cancer incidence is steadily rising worldwide (1). Chemotherapy has significantly improved survival outcomes in oncology (2). Doxorubicin (DOX) (Adriamycin), an anthracycline antibiotic, is widely used for treating both solid and hematological malignancies, including breast cancer, lymphomas, leukemias, and sarcomas (2,3). Despite its potent antitumor efficacy, the clinical utility of DOX is limited by its dose-dependent cardiotoxicity (4), which is often irreversible and may result in long-term cardiac morbidity (5). Preventing these side effects remains a key challenge in oncology.

DOX cardiotoxicity is multifactorial, with oxidative stress and inflammation playing central roles. In addition to mitochondrial oxidative injury, DOX promotes cardiomyocyte apoptosis and inflammatory signaling, thereby contributing to cardiac dysfunction (6). Notably, recent studies indicate that SIRT1 exerts cardioprotective effects through modulating cellular stress responses.

Flavonoid antioxidants have shown promise in mitigating DOX-induced toxicity. Quercetin (QRC), a natural flavonol found in various yellow and orange fruits and vegetables (7,8), exhibits anti-inflammatory, antioxidant, anticancer, and cytoprotective properties, attributed to its five hydroxyl groups (8-10). Experimental models suggest that QRC exerts cardioprotective effects by scavenging reactive oxygen species (ROS), enhancing antioxidant enzyme activity, and attenuating endoplasmic reticulum (ER) stress. However, while QRC's cardioprotective effects are promising, the precise mechanisms by which it confers protection, particularly its influence on less-studied pathways like ER stress in DOX-induced toxicity, remain to be determined.

We hypothesize that QRC exerts therapeutic effects against DOX-induced cardiotoxicity by modulating pathways including SIRT1, GRP78–CHOP, malondialdehyde (MDA)–glutathione (GSH), and tumor necrosis factor (TNF)-α–interleukin (IL)-6. This study aims to evaluate the cardioprotective potential of QRC through biochemical, scintigraphic, and electrocardiographic parameters. Furthermore, the use of clinically relevant diagnostic modalities—such as pyrophosphate (PYP) scintigraphy, serum troponin and creatine kinase (CK)- myocardial band (MB) levels, and electrocardiography (ECG)-derived conduction and arrhythmia metrics—may offer a novel translational approach.

Materials and Methods

Animal

All procedures were approved by the Local Animal Experiments Ethics Committee of Tokat Gaziosmanpaşa University (approval no: 2019-HADYEK-15, date: 09.06.2019). Male Wistar Albino rats were housed under standard laboratory conditions with ad libitum access to food and water and allowed a one-week acclimatization period before experimentation. This is an experimental animal study conducted in accordance with national and institutional guidelines for the care and use of laboratory animals.

Experimental groups and procedures

The animals were randomly allocated into four experimental groups, and the following procedures were applied:

Group I (Control group): Rats in the control group received no treatment throughout the experimental period.

Group II (DOX group): DOX was administered intraperitoneally (i.p) on experimental days 12, 13, and 14, at a cumulative dose of 18 mg/kg.

Group III (Low-dose QRC + DOX group; QRC 10 mg/kg + DOX): QRC was administered i.p at a dose of 10 mg/kg once daily for 14 consecutive days. In addition, DOX was injected (i.p) on days 12, 13, and 14 at a cumulative dose of 18 mg/kg.

Group IV (High-dose QRC + DOX group; QRC 100 mg/kg + DOX): QRC was administered i.p. at a dose of 100 mg/kg once daily for 14 consecutive days. DOX was additionally administered (i.p) on days 12, 13, and 14 at a cumulative dose of 18 mg/kg.

Scintigraphic imaging

For scintigraphic evaluation, 1 millicurie (mCi) of 99mTc-(99mTc-PYP) radiopharmaceutical (TechneScan PYP, Mallinckrodt) was diluted with 5 mL of isotonic saline, and 0.1 mL of the prepared solution was administered intravenously to each rat. One hour after injection, static planar scintigraphic imaging was performed with a gamma camera (Siemens Symbia, USA).

To facilitate scintigraphic imaging, rats were anesthetized with ketamine (Ketalar®, 75 mg/kg; Pfizer, İstanbul, Turkey) and xylazine (Rompun®, 10 mg/kg; Bayer, İstanbul, Turkey) administered at the indicated doses. Scintigraphic acquisition was conducted for 15 minutes under anesthesia.

Regions of interest (ROIs) were manually defined over the affected myocardial area, and seven separate measurements were obtained for each animal. The mean ROI value was calculated and used for quantitative analysis.

Radiation safety considerations

The 1 Technetium-99m pyrophosphate (99mTc-PYP) mCi dose used in rats in the present study, therefore, represents a relatively low activity level. Following completion of scintigraphic imaging, animals were kept in lead-shielded containers for 24 hours to allow radioactive decay and reduction of residual activity. Accordingly, no radiation exposure to personnel or the environment was anticipated during or after the experimental procedures.

Electrocardiographic recording

Following scintigraphic imaging, the depth of anesthesia in rats was assessed by measuring pedal withdrawal reflexes. Subsequently, needle electrodes were inserted subcutaneously into the right and left forelimbs and the left hind limb of each rat.

ECG recordings were obtained for 1 minute using a MP-150 multi-channel physiological data acquisition system (BIOPAC Systems Inc., USA) with the accompanying software (version 3.8). Changes in ECG patterns, including ST-segment elevation, QT interval duration, and heart rate, were analyzed (Figure 1).

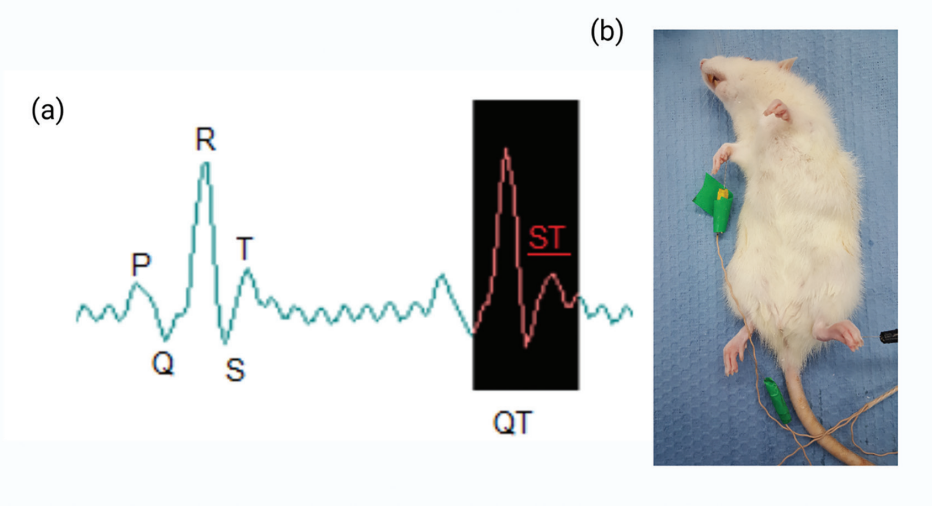

Figure 1. Electrocardiographic assessment in rats.

(a) Representative ECG waveform illustrating the P, QRS, and T waves, with indication of the QT interval and ST-segment elevation.

(b) Electrocardiographic recordings were obtained using a single-lead configuration (Lead II) with subcutaneous needle electrodes placed on the right and left forelimbs and the left hind limb

ECG: Electrocardiography, QT: Q wave-T wave interval

Quantification of Serum Cardiac, Renal, Hepatic Biomarkers and Cardiac Tissues

Serum markers of cardiac, renal, and hepatic injury [aspartate transaminase (AST), alanine transaminase (ALT), blood urea nitrogen (BUN), gamma-glutamyl transferase (GGT), CK-MB, creatinine, and cardiac troponin T (cTnT) were quantified using kinetic spectrophotometric assays on a Beckman Coulter LX-2000 autoanalyzer (Brea, CA, USA).

Cardiac tissues were homogenized in cold phosphate-buffered saline (pH 7.4), centrifuged, and the supernatants were analyzed. Tissue levels of SIRT1, MDA, GSH, TNF-α, IL-6, GRP78, and CHOP were quantified using ELISA. Results were normalized to wet tissue weight and expressed in appropriate units. Rats received QRC (10 or 100 mg/kg, i.p.) for 14 days, with DOX administered on days 12-14 (cumulative dose: 18 mg/kg, i.p.) (Figure 2).

Statistical Analysis

Statistical analyses were performed using SPSS software (version 19.0; IBM Corp., Armonk, NY, USA) and GraphPad Prism (version 10.0; GraphPad Software, San Diego, CA, USA). Data normality was assessed using the Shapiro-Wilk test. Variables that did not follow a normal distribution were analyzed using the Kruskal-Wallis test, followed by pairwise Mann-Whitney U tests with Bonferroni correction for multiple comparisons, including ^{99}mTc-PYP uptake, MDA, creatinine, and ALT. Normally distributed variables were analyzed using One-Way Analysis of Variance (ANOVA) followed by Tukey's post-hoc test. Data are presented as mean ± standard error of the mean (SEM) (mean ± SEM). A value of $p<0.05$ was considered statistically significant.

Results

Scintigraphic results

Kruskal-Wallis analysis revealed a significant overall difference among the groups in myocardial 99mTc-PYP uptake [$\chi^2(3) = 21.849$, $p<0.001$]. Consistent with this finding, myocardial radiotracer uptake was markedly increased in the DOX group compared with the control group ($p<0.0001$). Although myocardial 99mTc-PYP uptake remained higher than control values in both QRC-treated groups [DOX + QRC (10 mg/kg), $p<0.0001$; DOX + QRC (100 mg/kg), $p=0.0106$], direct comparison with the DOX group demonstrated a significant dose-dependent reduction in tracer accumulation (10 mg/kg: $p=0.0329$; 100 mg/kg: $p=0.0006$). Comparison between the two QRC-treated groups revealed that administration of 100 mg/kg QRC resulted in significantly lower myocardial radiotracer uptake than 10 mg/kg, indicating a dose-dependent effect ($p=0.0106$). These findings demonstrate that QRC administration significantly attenuates DOX-induced myocardial accumulation of 99mTc-PYP in a dose-dependent manner, suggesting a protective effect of QRC against DOX-related myocardial injury (Figure 3, Table 1).

Red circles indicate ROIs placed over the cardiac area for quantitative analysis. DOX administration resulted in markedly increased myocardial radiotracer accumulation compared with controls, whereas QRC treatment reduced myocardial 99mTc-PYP uptake in a dose-dependent manner.

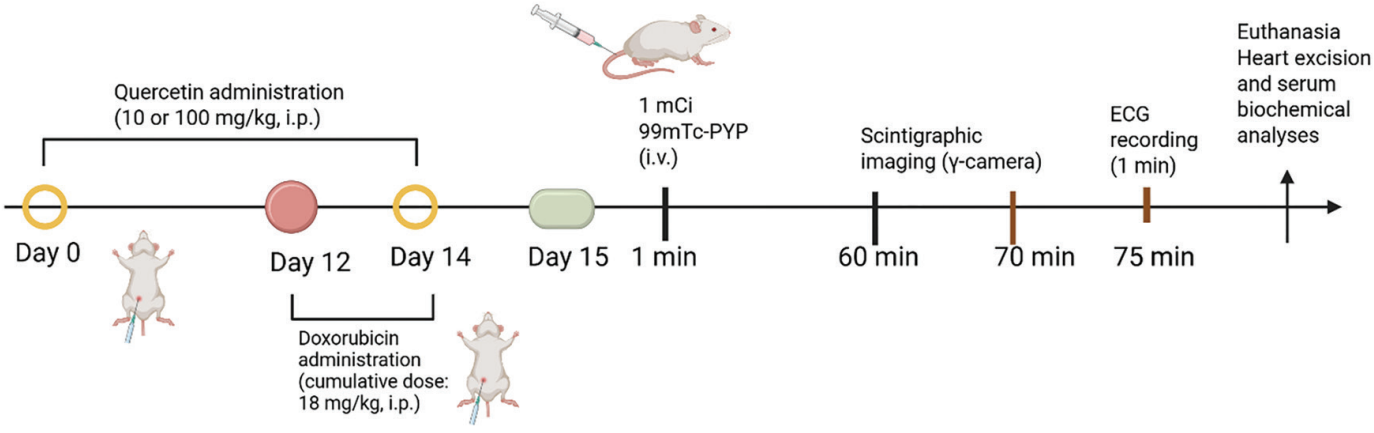

Figure 2. Experimental timeline
ECG: Electrocardiography, PYP: Pyrophosphate

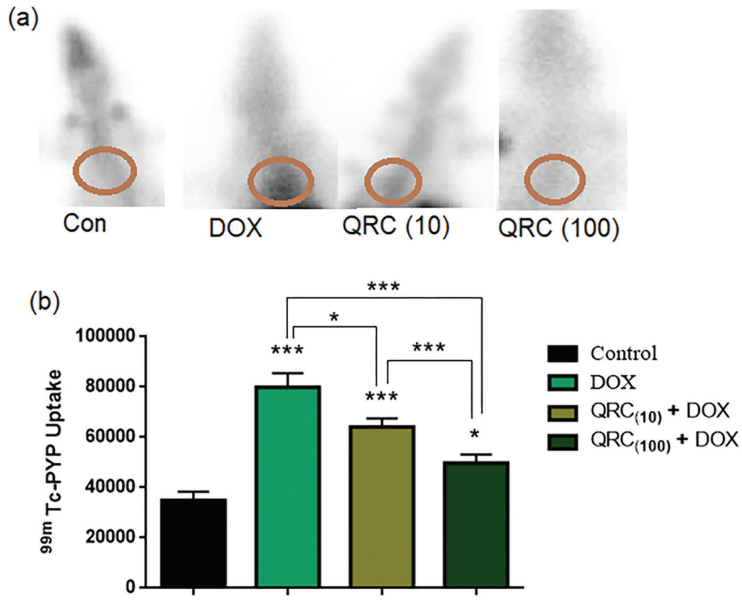

Figure 3. Effects of quercetin on doxorubicin-induced myocardial 99mTc-PYP uptake

Representative planar myocardial scintigraphic images obtained 1 h after intravenous injection of 99mTc-PYP are shown for the (a) Control, (b) DOX, (c) DOX + QRC (10 mg/kg), and (d) DOX + QRC (100 mg/kg) groups.

The lower panel shows quantitative analysis of myocardial ^{99}mTc-PYP uptake, expressed as mean ± SEM (n=7 per group). Differences among groups were analyzed using the Kruskal-Wallis test followed by pairwise Mann-Whitney U tests with Bonferroni correction for multiple comparisons

**: p<0.05, **: p<0.01, ***: p<0.001 were considered statistically significant, PYP: Pyrophosphate, DOX: Doxorubicin, SEM: Standard error of the mean, QRC: Quercetin*

Table 1. Scintigraphic and electrocardiographic findings in control and experimental groups

	Control	DOX	QRC (10) + DOX	QRC (100) + DOX
99mTc-PYP uptake	34914±3583	79943±5613[b]	64171±3365[b,c]	49829±3393[a,d,f]
Heart rate (bpm)	307±3.92	225±8.69 [b]	256±8.5[b,c]	293±4.18[d]
QT interval (duration, s)	0.070±0.002	0.110±0.006[b]	0.082±0.003[c]	0.075±0.003[d,e]
ST-segment amplitude (mV)	0.037±0.002	0.116±0.007[b]	0.068±0.003[b,d]	0.045±0.003[d,e]

[a]: p<0.05, [b]: p<0.001, all groups when compared to control group, [c]: p<0.05, [d]: p<0.001 QRC (10) + DOX and QRC (100) + DOX groups when compared to DOX group, [e]: p<0.01, [f]: p<0.001, QRC (10) + DOX group when compared to QRC (100) + DOX group.
Data are presented as mean ± SEM (n=7 per group). 99mTc-PYP uptake was analyzed using the Kruskal-Wallis test followed by pairwise Mann-Whitney U tests with Bonferroni correction for multiple comparisons. Electrocardiographic parameters (heart rate, QT interval, and ST-segment amplitude) were analyzed using One-Way ANOVA followed by Tukey's post-hoc test, DOX: Doxorubicin, SEM: Standard error of the mean, QT: Q wave-T wave interval, QRC: Quercetin

Effects on ECG parameters

Heart rate analysis revealed a significant overall group effect [F(3.24) =30.32, p<0.0001], with marked heart rate alteration in the DOX group compared with controls (p<0.0001), while both QRC doses significantly improved heart rate relative to DOX (10 mg/kg: p=0.0175; 100 mg/kg: p<0.0001), and the higher dose restored values to control levels (p=0.4687).

QT interval duration and ST segment elevation differed significantly among groups [QT: F(3.24) =18.42, p<0.0001; ST: F(3.24) =58.56, p<0.0001], with DOX inducing pronounced QT prolongation and ST elevation compared with controls (both p<0.0001). While QT interval prolongation was only partially reduced in the DOX + QRC (10 mg/kg) group and did not reach statistical significance compared with the DOX group (p=0.1935), treatment with DOX + QRC (100 mg/kg) resulted in a significant shortening of the QT interval (p<0.0001). ST-segment elevation was significantly attenuated in both QRC-treated groups compared with the DOX group (DOX + QRC 10 mg/kg, p=0.0005; DOX + QRC 100 mg/kg, p<0.0001). Notably, ST segment values were significantly lower in the DOX + QRC (100 mg/kg)

group than in the DOX + QRC (10 mg/kg) group (p=0.0098), indicating a dose-dependent cardioprotective effect (Figure 4, Table 1).

Biochemical Parameters

Serum cardiac injury markers (cTnT and CK-MB)

Data presented in Table 2 and Figure 5 revealed significant group differences in serum cardiac injury markers. One-Way ANOVA showed significant overall effects for both cTnT [F(3.24) =28.96, p<0.0001] and CK-MB [F(3.24) =22.75, p<0.0001]. Both markers were significantly elevated in the DOX group compared with controls (both p<0.0001), indicating marked myocardial injury.

Post-hoc Tukey analysis demonstrated that QRC treatment significantly reduced cTnT and CK-MB levels compared with the DOX group (cTnT: QRC 10 mg/kg, p=0.0005; QRC 100 mg/kg, p<0.0001; CK-MB: QRC 10 mg/kg, p=0.0016; QRC 100 mg/kg, p<0.0001). No significant differences were observed between the two QRC doses for either marker (cTnT, p=0.0289; CK-MB, p=0.1589), and biomarker levels in QRC-treated groups did not differ significantly from controls (p>0.05) (Figure 5, Table 2).

ER stress-related parameters (GRP78 and CHOP)

Data presented in Table 2 and Figure 6 show that ER stress-related markers were significantly affected by DOX treatment. One-Way ANOVA revealed significant overall group differences for both GRP78 [F(3.24) =16.65, p<0.0001] and CHOP [F(3.24) =106.0, p<0.0001]. Both GRP78 and CHOP levels were significantly increased in the DOX group compared with the control group (p<0.0001 for both), indicating pronounced ER stress induction following DOX administration (Figure 6, Table 2).

Administration of QRC at both doses significantly reduced GRP78 content and CHOP activity compared with the DOX group (QRC 10 mg/kg: GRP78 p=0.0244, CHOP p<0.0001; QRC 100 mg/kg: GRP78 p=0.0002, CHOP p<0.0001). When the two QRC doses were compared, no statistically significant difference was observed in GRP78 levels

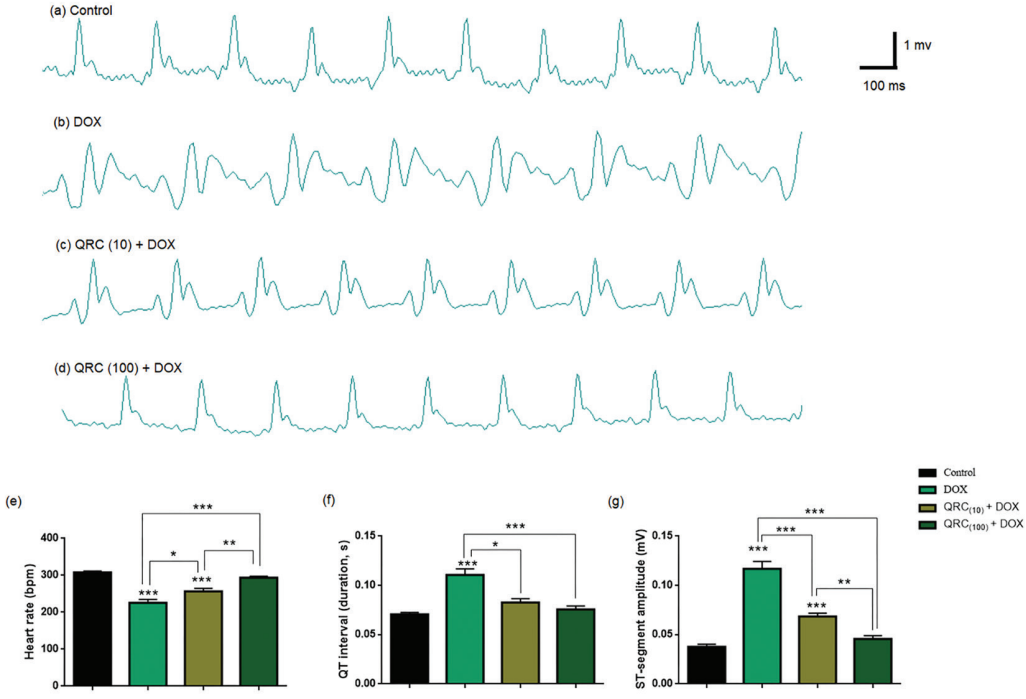

Figure 4. Effects of quercetin on doxorubicin-induced electrocardiographic alterations

Representative electrocardiographic (ECG) recordings obtained from rats in the (a) Control, (b) DOX, (c) DOX + QRC (10 mg/kg), and (d) DOX + QRC (100 mg/kg) groups are shown.

Quantitative analyses of (e) heart rate, (f) QT interval duration, and (g) ST segment amplitude are presented as mean ± SEM (n=7 per group). Statistical comparisons were performed using One-Way ANOVA followed by Tukey's multiple comparisons test

**: p<0.05, **: p<0.01, ***: p<0.001 indicate significant differences between groups, as specified, DOX: Doxorubicin, QRC: Quercetin, QT: Q wave-T wave interval*

(p=0.1923), whereas CHOP levels were significantly lower in the QRC (100 mg/kg) group than in the QRC (10 mg/kg) group (p<0.0001), indicating a dose-dependent attenuation of CHOP-mediated ER stress and apoptotic signaling.

Oxidative stress-related parameters (MDA and GSH)

Kruskal-Wallis analysis revealed a significant overall difference among the groups in MDA levels [$\chi^2(3) = 19.619$, p<0.001]. Consistent with this finding, MDA levels were significantly increased in the DOX group compared with the control group (p<0.0001), indicating enhanced lipid peroxidation. QRC treatment significantly reduced MDA levels compared with the DOX group (QRC 10 mg/kg, p=0.002; QRC 100 mg/kg, p<0.0001). In parallel, reduced GSH levels showed a significant overall group effect by One-Way ANOVA [F(3.24) =28.01, p<0.0001], with a marked decrease observed in the DOX group relative to controls (p<0.0001). QRC administration significantly increased GSH levels in both treatment groups (QRC 10 mg/kg and QRC 100 mg/kg, p=0.024, p<0.0001, respectively). Notably, MDA levels were significantly lower in the QRC (100 mg/kg) group than in the QRC (10 mg/kg) group (p=0.0148), whereas no significant difference was observed in GSH levels between the two QRC-treated groups (p>0.05) (Figure 6, Table 2).

Table 2. Biochemical parameters in heart tissue and serum

	Control	DOX	QRC (10) + DOX	QRC (100) + DOX
cTnT (pg/mL)	785±221	3731±418[c]	2091±126[b,f]	1031±88[f,g]
CK-MB (U/L)	462±26	868±37[c]	646±22[b,e]	531±54[f]
GRP78 (ng/mg protein)	0.73±0.07	2.13±0.23[c]	1.49±0.13[b,d]	1.05±0.10[f]
CHOP (pg/mg protein)	44.77±3.10	182.5±7.40[c]	127±6.89[c,f]	77.32±4.94[b,f,h]
TNF-a (pg/mg)	128±10	282±27[c]	170±17[f]	125±11[f]
IL-6 (pg/mg)	4.96±0.58	11.10±0.99[c]	6.92±0.85[e]	5.16±0.56[f]
MDA (nmol/mg)	1.60±0.15	5.17±0.43[c]	2.91±0.29[b,e]	1.92±0.18[f,g]
GSH (µmol/g)	47.87±2.47	18.43±1.61[c]	28.76±2.89[c,d]	37.29±2.29[a,f]
SIRT1 (ng/mg)	3.40±0.15	1.45±0.06[c]	2.21±0.18[c,d]	2.76±0.23[f]

[a]: p<0.05, [b]: p<0.01, [c]: p<0.001, all groups when compared to control group, [d]: p<0.05, [e]: p<0.01, [f]: p<0.001, QRC (10) + DOX and QRC (100) + DOX groups when compared to DOX group, [g]: p<0.05, [h]: p<0.001 QRC (10) + DOX group when compared to QRC (100) + DOX group, data are presented as mean ± SEM (n=7 per group) DOX: Doxorubicin, GSH: Glutathione, QRC: Quercetin, MDA: Malondialdehyde, CK-MB: Creatine kinase-myocardial band, TNF: Tumor necrosis factor, SEM: Standard error of the mean

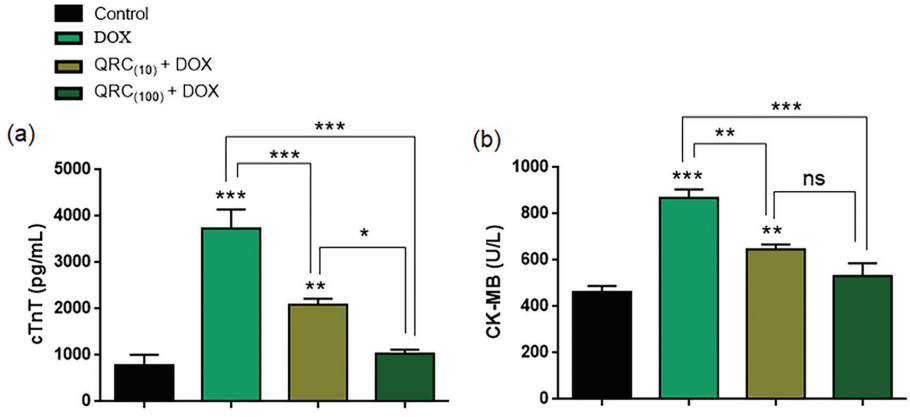

Figure 5. Serum cardiac injury markers. (a) cTnT and (b) CK-MB levels in control, DOX, QRC (10 mg/kg) + DOX, and QRC (100 mg/kg) + DOX groups. Data are presented as mean ± SEM (n=7). Statistical analysis was performed using One-Way ANOVA followed by Tukey's post-hoc test

**: p<0.05, **: p<0.01, ***: p<0.001, ns: Not significant, DOX: Doxorubicin, QRC: Quercetin, CK-MB: Creatine kinase-myocardial band, cTnT: Cardiac troponin T, SEM: Standard error of the mean*

Inflammation-related cytokines (TNF-α and IL-6)

Data presented in Table 2 and Figure 7 demonstrate significant alterations in pro-inflammatory cytokine levels among the experimental groups. One-Way ANOVA revealed significant overall group differences for both TNF-α [F(3.24) =16.97, p<0.0001] and IL-6 [F(3.24) =13.55, p<0.0001]. TNF-α and IL-6 levels were significantly increased in the DOX group compared with the control group (both 0.0001), indicating a pronounced inflammatory response following DOX administration. QRC treatment significantly reduced TNF-α and IL-6 levels compared with the DOX group at both doses (TNF-α: QRC 10 mg/kg p=0.0009, QRC 100 mg/kg p<0.0001; IL-6: QRC 10 mg/kg p=0.0044, QRC 100 mg/kg p<0.0001). However, no statistically significant difference was observed between the two QRC-treated groups for either TNF-α (p=0.3131) or IL-6 (p=0.3912) (Figure 7, Table 2).

SIRT1

Data presented in Table 2 and Figure 7 demonstrate significant alterations in SIRT1 levels among the experimental groups. One-Way ANOVA revealed a significant overall group effect for SIRT1 [F(3.24) =23.64, p<0.0001]. SIRT1 levels were significantly reduced in the DOX group compared with the control group (p<0.0001), indicating suppression of SIRT1–mediated cytoprotective signaling following DOX administration (Figure 7, Table 2).

QRC treatment significantly restored SIRT1 levels compared with the DOX group at both doses (QRC 10 mg/kg, p=0.0218; QRC 100 mg/kg, p<0.0001). However, no statistically significant difference was observed between the two QRC-treated groups (p=0.1274), suggesting that QRC-induced SIRT1 activation was not dose-dependent under the present experimental conditions.

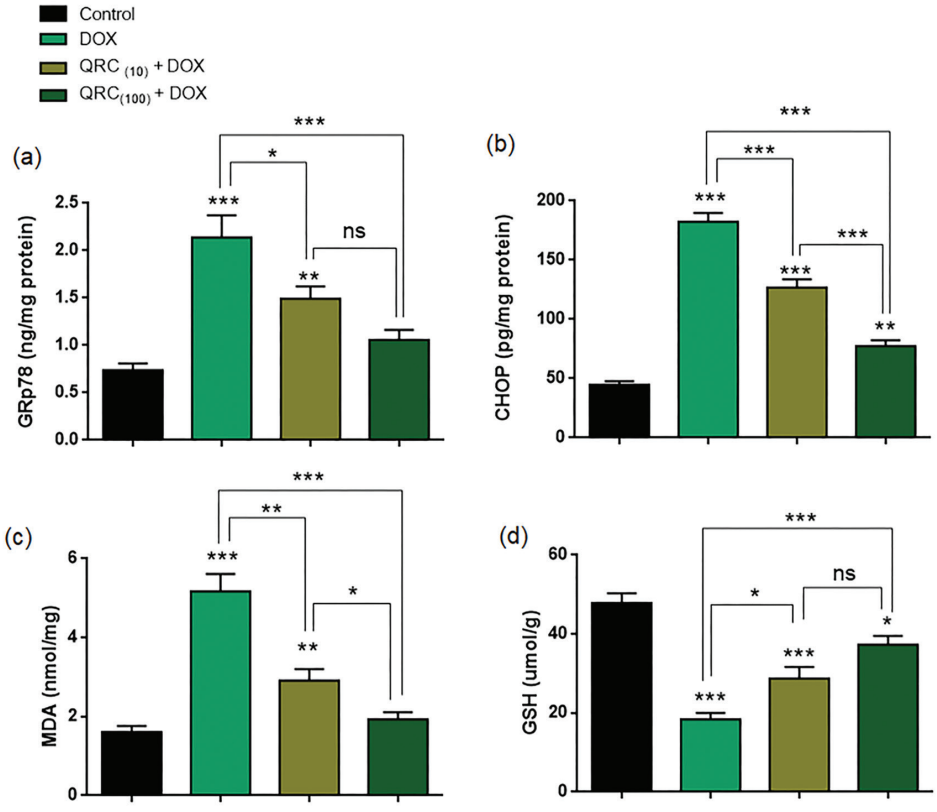

Figure 6. Effects of quercetin on ER stress and oxidative stress markers in cardiac tissue. Levels of (a) GRP78, (b) CHOP, (c) malondialdehyde (MDA), and (d) reduced (GSH) in control, DOX, QRC (10 mg/kg) + DOX, and QRC (100 mg/kg) + DOX groups. Data are expressed as mean ± SEM (n=7 per group).

GRP78, CHOP, and GSH were analyzed using One-Way ANOVA followed by Tukey's post-hoc test, whereas MDA levels were analyzed using the Kruskal-Wallis test followed by pairwise Mann-Whitney U tests with Bonferroni correction for multiple comparisons

**: p<0.05, **: p<0.01, ***: p<0.001, ns: Not significant, GSH: Glutathione, DOX: Doxorubicin, QRC: Quercetin, ER: Endoplasmic reticulum, CHOP: C/EBP homologous protein, SEM: Standard error of the mean*

Normally distributed variables were analyzed using One-Way ANOVA followed by Tukey's post-hoc test. Non-normally distributed variables (MDA) were analyzed using the Kruskal-Wallis test followed by pairwise Mann-Whitney U tests with Bonferroni correction for multiple comparisons.

Biochemical renal and hepatic markers

Renal Function Markers: BUN and Creatinine

BUN values showed a normal distribution. They were therefore analyzed using One-Way ANOVA, which revealed a significant overall group effect [$F(3.24) = 48.04$, $p<0.0001$], indicating that DOX administration significantly increased BUN levels compared with the Control group ($p<0.0001$), while co-treatment with QRC at 10 mg/kg (QRC 10 + DOX) and 100 mg/kg (QRC 100 + DOX) significantly attenuated this increase relative to the DOX group ($p<0.001$ and $p<0.001$, respectively), with no significant difference between the two QRC doses ($p=0.069$).

In contrast, serum creatinine levels did not follow a normal distribution and were therefore analyzed using the Kruskal-Wallis test, which revealed a significant overall difference among the groups [$\chi^2(3) = 23.485$, $p<0.001$]. Pairwise comparisons demonstrated that DOX significantly increased creatinine levels compared with the control group ($p<0.0001$). Treatment with QRC significantly reduced creatinine levels relative to the DOX group in both treatment groups (QRC 10 + DOX, $p=0.0379$; QRC 100 + DOX, $p<0.0001$). Moreover, creatinine levels were significantly lower in the QRC 100 + DOX group than in the QRC 10 + DOX group ($p=0.0015$), indicating a stronger protective effect at the higher dose.

Hepatic Enzymes: AST, ALT, and GGT

As shown in Table 3 and Figure 8, normality testing indicated that AST and GGT values were normally distributed, and these variables were therefore analyzed using One-Way ANOVA. A significant overall treatment effect was observed for AST [$F(3.24) = 27.91$, $p<0.0001$] and GGT [$F(3.24) = 33.41$, $p<0.0001$]. Post-hoc Tukey's multiple comparisons test demonstrated that DOX administration markedly increased serum AST and GGT levels compared with the control group (both $p<0.001$), indicating pronounced hepatocellular injury (Figure 8).

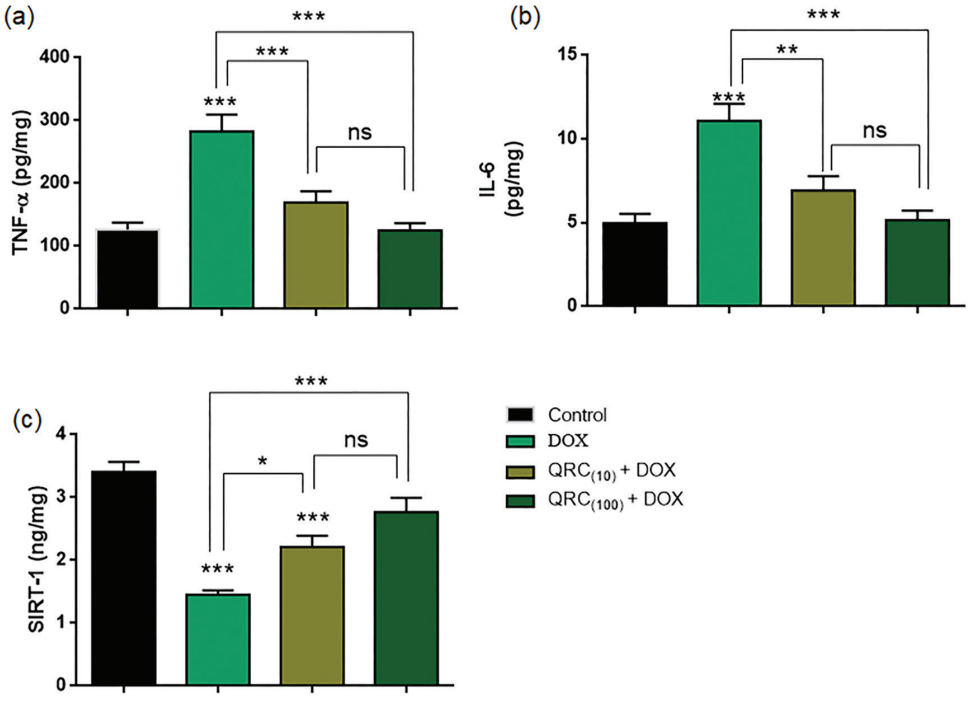

Figure 7. Effects of quercetin on inflammatory and SIRT1 signaling markers in cardiac tissue. (a) TNF-α, (b) IL-6, and (c) SIRT1 levels in control, DOX, QRC (10 mg/kg) + DOX, and QRC (100 mg/kg) + DOX groups. Data are expressed as mean ± SEM (n=7). One-Way ANOVA followed by Tukey's post-hoc test

**: p<0.05, **: p<0.01, ***: p<0.001, ns: Not significant, SEM: Standard error of the mean, TNF: Tumor necrosis factor, DOX: Doxorubicin, QRC: Quercetin*

Table 3. Renal and hepatic biochemical markers

	Control	DOX	QRC (10) + DOX	QRC (100) + DOX
Creatinine (mg/dL)	0.40±0.02	2.11±0.20[c]	1.54±0.14[c,d]	0.86±0.08[c,f,g]
BUN (mg/dL)	25.14±1.42	97.43±6.84[c]	64.43±4.19[c,f]	48.29±3.21[b,f]
AST (U/L)	191.9±8.54	581.6±48.71[c]	407.4±24.74[c,e]	300±29.96[f]
ALT (U/L)	62±2.58	287.6±24.24[b]	192.1±14.21[b,d]	139.1±5.0[b,e,g]
GGT (U/L)	5.28±0.42	18.71±1.16[c]	13.14±1.26[c,e]	9.85±0.82[a,f]

[a]: p<0.05, [b]: **p<0.01, [c]: *** p<0.001 vs. control; [d]: p<0.05, [e]: **p<0.01, [f]: ***p<0.001 vs. DOX;
[g]: p<0.01 QRC (10) + DOX group when compared to QRC (100) + DOX, DOX: Doxorubicin, QRC: Quercetin, BUN: Blood urea nitrogen, AST: Aspartate transaminase, ALT: Alanine transaminase, GGT: Gamma-glutamyl transferase

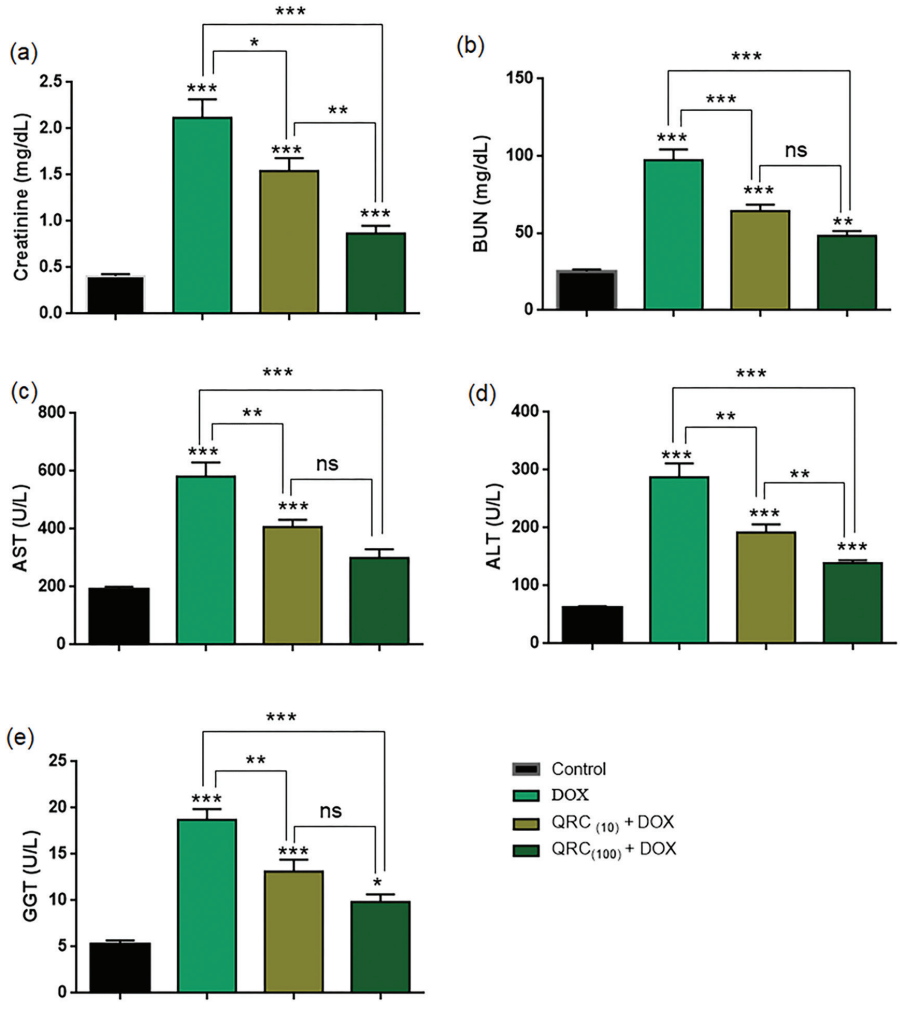

Figure 8. Effects of quercetin on doxorubicin-induced renal and hepatic injury markers.

Serum levels of (a) creatinine (mg/dL), (b) blood urea nitrogen [(BUN), mg/dL], (c) aspartate aminotransferase [(AST), U/L], (d) alanine aminotransferase [(ALT), U/L], and (e) gamma-glutamyl transferase [(GGT), U/L] in Control, doxorubicin (DOX), QRC 10 mg/kg + DOX [QRC (10) + DOX], and QRC 100 mg/kg + DOX (QRC (100) + DOX) groups. One-Way ANOVA followed by Tukey's multiple comparisons test was used for normally distributed variables (BUN, AST, and GGT). ALT and creatinine values were analyzed using the Kruskal-Wallis test followed by Mann-Whitney U post-hoc comparisons, *: p<0.05, **: p<0.01, ***: p<0.001 vs. control;

Brackets indicate comparisons between treatment groups; ns: Not significant.

Normally distributed variables were analyzed using One-Way ANOVA followed by Tukey's post-hoc test. Non-normally distributed variables (ALT and creatinine) were analyzed using the Kruskal-Wallis test followed by pairwise Mann-Whitney U tests with Bonferroni correction for multiple comparisons

Co-treatment with QRC at 10 mg/kg (QRC 10 + DOX) significantly attenuated the DOX-induced elevations in AST (p=0.0003) and GGT (p=0.0026) relative to the DOX group. Similarly, QRC at 100 mg/kg (QRC 100 + DOX) produced a more pronounced reduction in AST and GGT (both p<0.001) compared with DOX alone. Direct comparison between QRC 10 + DOX and QRC 100 + DOX revealed no statistically significant difference for AST (p=0.1016) or GGT (p=0.1090).

In contrast, serum ALT values did not follow a normal distribution and were therefore analyzed using the Kruskal-Wallis test, which demonstrated a significant overall difference among the experimental groups [$\chi^2(3) = 24.416$, p<0.001].

ALT levels were significantly higher in the DOX group compared with the control group (p=0.002). QRC treatment significantly reduced ALT levels relative to the DOX group in both treatment groups (QRC 10 + DOX, p=0.013; QRC 100 + DOX, p=0.002). Furthermore, ALT levels were significantly lower in the DOX + QRC (100 mg/kg) group than in the DOX + QRC (10 mg/kg) group (p=0.002), indicating a dose-dependent hepatoprotective effect of QRC.

Discussion

In the present study, DOX administration induced marked ER stress and oxidative-inflammatory damage in cardiac tissue, as evidenced by increased GRP78, CHOP, MDA, TNF-α, and IL-6 levels together with reduced SIRT1 and GSH, which were paralleled by significant electrocardiographic abnormalities and increased myocardial uptake on Tc-99m PYP scintigraphy. Notably, QRC dose-dependently attenuated these biochemical, electrophysiological, and scintigraphic alterations, with the higher dose conferring more pronounced cardioprotection.

In this study, Electrocardiographic analysis revealed significant QT interval prolongation, ST-segment elevation, and bradycardia in the DOX-treated rat. QT prolongation is a well-established marker of impaired ventricular repolarization and is closely associated with malignant arrhythmias and increased cardiovascular mortality (11,12). DOX has been shown to prolong cardiac action potential duration by disrupting delayed rectifier potassium currents (IKr/IKs) and calcium handling (13,14). At the same time, the accompanying ST-segment elevation likely reflects myocardial membrane injury and necrosis-related injury currents. The accompanying reduction in heart rate may be attributed to DOX-induced sinus node dysfunction and autonomic imbalance, which have previously been linked to mitochondrial damage and oxidative stress in pacemaker cells (15,16).

Tc-99m PYP is a radiopharmaceutical that binds to calcium complexes and preferentially accumulates in necrotic tissue. It has been routinely used in nuclear medicine for the imaging of myocardial and tissue necrosis (17-20). Consistent with this study, diffuse myocardial PYP uptake occurs in anthracycline-injured hearts (21). Miyagawa et al. (22) evaluated chronic DOX-induced myocardial injury in a rat model using 201Tl-thallium and ^{99}mTc-PYP uptake. They reported that cardiac accumulation of ^{99}mTc-PYP occurred only in the presence of advanced necrotic myocardial damage. In the present study, PYP uptake was markedly reduced in QRC-treated groups compared to DOX alone, indicating that QRC mitigated DOX-induced myocardial injury and supporting its cardioprotective role.

Consistent with the ECG and scintigraphic findings, DOX administration resulted in marked elevations in serum cTnT and CK-MB levels, confirming substantial cardiomyocyte injury and membrane disruption. Troponin elevation is widely accepted as a sensitive indicator of anthracycline-induced myocardial damage and has been correlated with both acute and long-term cardiac dysfunction (23). Consistent with previous reports, DOX administration resulted in significant elevations in cTnT and CK-MB levels, confirming myocardial injury (24,25).

DOX-induced oxidative stress primarily arises from excessive ROS generation during mitochondrial metabolism in cardiomyocytes, which are particularly susceptible due to their high mitochondrial density and limited antioxidant capacity (26,27). Excess ROS damages lipid membranes, proteins, and nucleic acids, promoting cardiomyocyte dysfunction and death (28), while simultaneously triggering inflammatory signaling. In this context, DOX has been shown to activate NF-κB, TLR4, and the NLRP3 inflammasome, leading to increased TNF-α and IL-6 production (29,30), consistent with the elevated cytokine levels observed in the present study. Oxidative stress is also closely linked to ER stress, as ROS disrupts protein folding and activates the unfolded protein response. The concurrent upregulation of GRP78 and CHOP suggests a shift toward ER stress–mediated apoptosis, consistent with reports of CHOP-dependent cardiomyocyte death in DOX models (31).

In the current study, the observed reduction in SIRT1 expression in DOX-treated hearts provides important mechanistic insight into DOX cardiotoxicity. SIRT1 is a NAD^+-dependent deacetylase that plays a central role in

cellular stress adaptation, and previous studies have shown that DOX exposure suppresses cardiac SIRT1 expression and activity, thereby enhancing ROS generation and myocardial injury (32,33). Under physiological conditions, SIRT1 negatively regulates both ER stress and inflammatory signaling by modulating UPR activity and limiting NF-κB-dependent cytokine transcription (34). Thus, DOX-mediated SIRT1 suppression likely contributes to sustained ER stress activation and increased TNF-α and IL-6 production. Supporting this interpretation, experimental models have demonstrated that SIRT1 deficiency markedly increases GRP78 and CHOP expression, whereas SIRT1 overexpression attenuates ER stress responses (35). Moreover, cardiomyocyte-specific SIRT1 deletion has been shown to activate multiple UPR branches and promote CHOP-dependent cell death (36), findings further corroborated in sepsis and aging models (37,38). Collectively, these data indicate that SIRT1 functions as a key negative regulator of the ER stress–UPR–CHOP axis in the heart.

QRC treatment markedly reversed the pathological alterations induced by DOX in the present study. QRC-treated groups exhibited significant reductions in GRP78 and CHOP expression, restoration of SIRT1 levels, attenuation of lipid peroxidation, and recovery of GSH content. In parallel, TNF-α and IL-6 levels were substantially reduced. These findings indicate that QRC simultaneously targets oxidative, ER, and inflammatory stress. Extensive evidence supports QRC's potent antioxidant capacity and cardioprotective efficacy across diverse cardiac injury models, including ischemia-reperfusion injury, myocardial infarction, and diabetic cardiomyopathy (39-43).

Mechanistically, QRC activates the Nrf2 signaling pathway, leading to enhanced expression of endogenous antioxidant defenses, including SOD, GSH, and HO-1 (44-46). Concurrently, QRC suppresses stress-activated inflammatory pathways by inhibiting NF-κB signaling, thereby reducing pro-inflammatory cytokine production. Notably, emerging evidence indicates that QRC can also enhance SIRT1 activity. Through SIRT1-dependent mechanisms, including XBP1 deacetylation, QRC dampens excessive UPR activation and alleviates ER stress (47-49).

In the present study, DOX administration significantly increased renal and hepatic injury markers, whereas QRC co-treatment partially but significantly reversed these alterations in a dose-dependent manner. Consistent with our findings, numerous experimental studies have demonstrated that DOX induces marked renal and hepatic dysfunction – reflected by elevations in serum creatinine, BUN, and hepatic transaminases – primarily through mechanisms involving oxidative stress, ER stress, and inflammatory signaling (50,51). Previous reports have shown that various antioxidant agents attenuate DOX-induced renal and hepatic injury by suppressing oxidative damage, reducing ER stress responses, and limiting inflammatory cascades (31,52). Several previous experimental studies have demonstrated that QRC protects against DOX-induced hepatic and renal toxicity by reducing oxidative stress and associated tissue damage in animal models (53-56). In line with this evidence, the observed renoprotective and hepatoprotective effects of QRC in our study may be, at least in part, attributed to its strong antioxidant properties, which likely mitigate DOX-induced oxidative and inflammatory tissue injury (Figure 9) (53-56).

Conclusion

These findings suggest that QRC interrupts the self-perpetuating cycle of ROS accumulation, ER stress, and DOX-induced inflammation. By restoring SIRT1 signaling and reinforcing antioxidant defenses, QRC preserves cellular homeostasis and limits cardiomyocyte injury. This integrated mechanism provides a coherent explanation for the observed cardioprotective effects of QRC in DOX-induced cardiotoxicity.

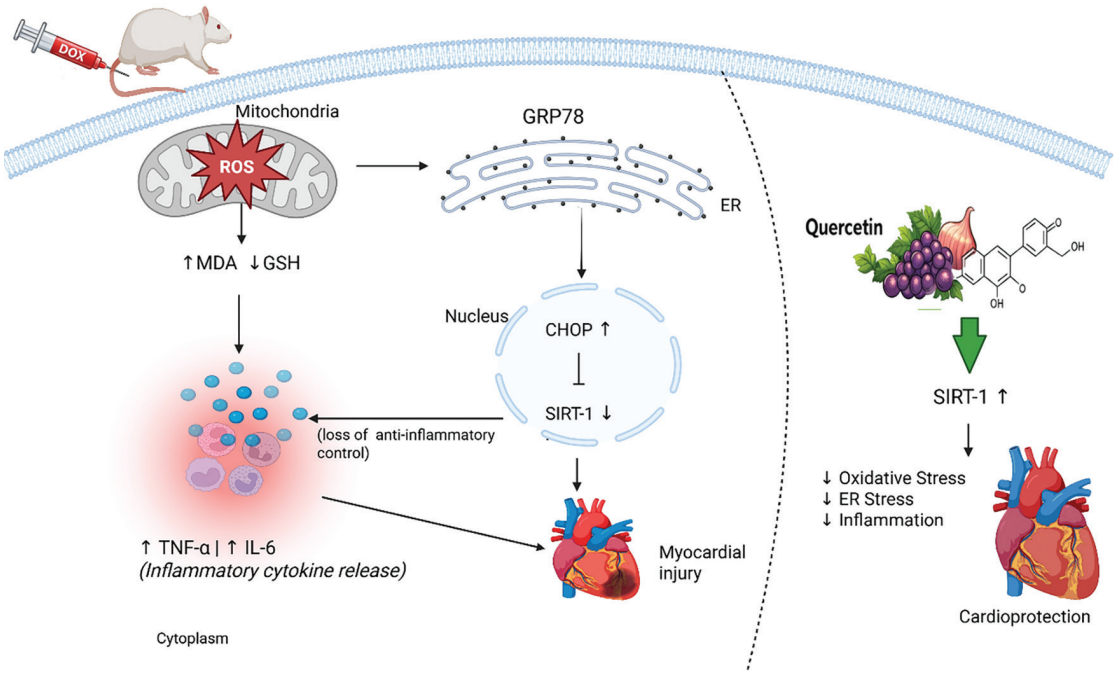

Figure 9. Graphical abstract

TNF: Tumor necrosis factor, MDA: Malondialdehyde, IL: Interleukin, ER: Endoplasmic reticulum, GSH: Glutathione, ROS: Reactive oxygen species

Ethics

Ethics Committee Approval: All procedures were approved by the Local Animal Experiments Ethics Committee of Tokat Gaziosmanpaşa University (approval no: 2019-HADYEK-15, date: 09.06.2019).

Informed Consent: Not applicable. This study is an experimental animal study.

Footnotes

Authorship Contributions

Surgical and Medical Practices: M.S., H.Y., G.E., M.K., S.S.G., F.D., A.A., H.A., Concept: M.S., H.A., Design: M.S., M.K., S.S.G., A.A., Data Collection or Processing: M.S., H.Y., G.E., M.K., S.S.G., F.D., A.A., H.A., Analysis or Interpretation: H.Y., G.E., M.K., S.S.G., F.D., H.A., Literature Search: H.Y., G.E., A.A., H.A., Writing: M.S., M.K., A.A.

Conflict of Interest: No conflict of interest was declared by the authors.

Financial Disclosure: The authors declared that this study received no financial support.

References

1. World Health Organization. Global cancer burden growing, amidst mounting need for services. [Internet]. (cited 2024 Feb 1). Available from:https://www.who.int/news/item/01-02-2024-global-cancer-burden-growing--amidst-mounting-need-for-services
2. Sun M, Zhang X, Tan B, Zhang Q, Zhao X, Dong D. Potential role of endoplasmic reticulum stress in doxorubicin-induced cardiotoxicity-an update. Front Pharmacol. 2024;15:1415108.
3. Darrabie MD, Arciniegas AJ, Mantilla JG, Mishra R, Vera MP, Santacruz L, et al. Exposing cardiomyocytes to subclinical concentrations of doxorubicin rapidly reduces their creatine transport. Am J Physiol Heart Circ Physiol. 2012;303(5):H539-H548.
4. Li DL, Hill JA. Cardiomyocyte autophagy and cancer chemotherapy. J Mol Cell Cardiol. 2014;71:54-61.
5. Mitry MA, Edwards JG. Doxorubicin induced heart failure: phenotype and molecular mechanisms. Int J Cardiol Heart Vasc. 2016;10:17-24.
6. Sun J, Sun G, Meng X, Wang H, Luo Y, Qin M, et al. Isorhamnetin protects against doxorubicin-induced cardiotoxicity in vivo and in vitro. PLoS One. 2013;8(5):e64526.
7. Yuksel Y, Yuksel R, Yagmurca M, Haltas H, Erdamar H, Toktas M, et al. Effects of quercetin on methotrexate-induced nephrotoxicity in rats. Hum Exp Toxicol. 2017;36(1):51-61.
8. Rashidi Z, Khosravizadeh Z, Talebi A, Khodamoradi K, Ebrahimi R, Amidi F. Overview of biological effects of quercetin on ovary. Phytother Res. 2021;35(1):33-49.
9. Najafi M, Tavakol S, Zarrabi A, Ashrafizadeh M. Dual role of quercetin in enhancing the efficacy of cisplatin in chemotherapy

and protection against its side effects: a review. Arch Physiol Biochem. 2022;128(6):1438-1452.

10. Onuoha SC, Ezim OE, Chisom NE, Chukwuebuka CB, Abarikwu SO. Combined protective effects of quercetin, rutin, and gallic acid against cadmium-induced testicular damages in young-adult rats. Andrologia. 2023;(1):9787664.

11. Zhang Y, Post WS, Blasco-Colmenares E, Dalal D, Tomaselli GF, Guallar E. Electrocardiographic QT interval and mortality: a meta-analysis. Epidemiology. 2011;22(5):660-670.

12. Porta-Sánchez A, Gilbert C, Spears D, Amir E, Chan J, Nanthakumar K, et al. Incidence, diagnosis, and management of QT prolongation induced by cancer therapies: a systematic review. J Am Heart Assoc. 2017;6(12):e007724.

13. Ducroq J, Moha ou Maati H, Guilbot S, Dilly S, Laemmel E, Pons-Himbert C, et al. Dexrazoxane protects the heart from acute doxorubicin-induced QT prolongation: a key role for I(Ks). Br J Pharmacol. 2010;159(1):93-101.

14. Bhutani V, Varzideh F, Wilson S, Kansakar U, Jankauskas SS, Santulli G. Doxorubicin-induced cardiotoxicity: a comprehensive update. J Cardiovasc Dev Dis. 2025;12(6):207. Erratum in: J Cardiovasc Dev Dis. 2025;12(7):242.

15. Qi JY, Yang YK, Jiang C, Zhao Y, Wu YC, Han X, et al. Exploring the mechanism of danshensu in the treatment of doxorubicin-induced cardiotoxicity based on network pharmacology and experimental evaluation. Front Cardiovasc Med. 2022;9:82797.

16. Kobayashi K, Nakatani M, Harada Y, Suzuki Y, Fukunishi N, Boché A, et al. Doxorubicin-induced sinus node dysfunction associated with mitochondria and nuclear impairment in a mouse model. J Physiol Sci. 2025;75(3):100047.

17. Isoda H, Itagaki Y, Nomura N, Urushida T, Naitou A, Watanabe A, et al. Usefulness of dual SPECT with Tc-99m pyrophosphate and Tl-201 to predict further events after acute myocardial infarction with single-vessel coronary artery disease. Clin Nucl Med. 1999;24(4):227-231.

18. Mochizuki T, Murase K, Higashino H, Miyagawa M, Sugawara Y, Kikuchi T, et al. Ischemic "memory image" in acute myocardial infarction of 123I-BMIPP after reperfusion therapy: a comparison with 99mTc-pyrophosphate and 201Tl dual-isotope SPECT. Ann Nucl Med. 2002;16(8):563-568.

19. Okuda K, Nohara R, Ogino M, Tamaki N, Konishi J, Fujita M, et al. Limitation of infarct size with preconditioning and calcium antagonist (diltiazem): difference in 99mTc-PYP uptake in the myocardium. Ann Nucl Med. 1996;10(2):201-209.

20. Einstein AJ, Shuryak I, Castaño A, Mintz A, Maurer MS, Bokhari S. Estimating cancer risk from ^{99m}Tc pyrophosphate imaging for transthyretin cardiac amyloidosis. J Nucl Cardiol. 2020;27(1):215-224.

21. Aygun H, Gul SS. Cardioprotective effect of melatonin and agomelatine on doxorubicin-induced cardiotoxicity in a rat model: an electrocardiographic, scintigraphic and biochemical study. Bratisl Lek Listy. 2019;120(4):249-255.

22. Miyagawa M, Tanada S, Hamamoto K. Scintigraphic evaluation of myocardial uptake of thallium 201 and technetium 99m pyrophosphate utilizing a rat model of chronic doxorubicin cardiotoxicity. Eur J Nucl Med. 1991;18(5):332-338.

23. Wettersten N, Maisel A. Role of cardiac troponin levels in acute heart failure. Card Fail Rev. 2015;1(2):102-106.

24. Hu C, Zhang X, Wei W, Zhang N, Wu H, Ma Z, et al. Matrine attenuates oxidative stress and cardiomyocyte apoptosis in doxorubicin-induced cardiotoxicity via maintaining AMPKα/UCP2 pathway. Acta Pharm Sin B. 2019;9(4):690-701.

25. Dulf PL, Coadă CA, Florea A, Moldovan R, Baldea I, Dulf DV, et al. Mitigating doxorubicin-induced cardiotoxicity through quercetin intervention: an experimental study in rats. Antioxidants (Basel). 2024;13(9):1068.

26. Minotti G, Menna P, Salvatorelli E, Cairo G, Gianni L. Anthracyclines: molecular advances and pharmacologic developments in antitumor activity and cardiotoxicity. Pharmacol Rev. 2004;56(2):185-229.

27. Jean SR, Tulumello DV, Riganti C, Liyanage SU, Schimmer AD, Kelley SO. Mitochondrial targeting of doxorubicin eliminates nuclear effects associated with cardiotoxicity. ACS Chem Biol. 2015;10(9):2007-2015.

28. Arrigoni R, Jirillo E, Caiati C. Pathophysiology of doxorubicin-mediated cardiotoxicity. Toxics. 2025;13(4):277.

29. Alwaili MA, Abu-Almakarem AS, El-Said KS, Eid TM, Mobasher MA, Alsabban AH, et al. Shikimic acid protects against doxorubicin-induced cardiotoxicity in rats. Sci Rep. 2025;15(1):8126.

30. Botros SR, Matouk AI, Amin A, Heeba GH. Comparative effects of incretin-based therapy on doxorubicin-induced nephrotoxicity in rats: the role of SIRT1/Nrf2/NF-κB/TNF-α signaling pathways. Front Pharmacol. 2024;15:1353029.

31. Zobeydi AM, Mousavi Namavar SN, Sadeghi Shahdani M, Choobineh S, Kordi MR, Rakhshan K. Mitigating doxorubicin-induced hepatotoxicity in male rats: the role of aerobic interval training and curcumin supplementation in reducing oxidative stress, endoplasmic reticulum stress and apoptosis. Sci Rep. 2025;15(1):6604. Erratum in: Sci Rep. 2025;15(1):12004.

32. Cappetta D, Esposito G, Piegari E, Russo R, Ciuffreda LP, Rivellino A, et al. SIRT1 activation attenuates diastolic dysfunction by reducing cardiac fibrosis in a model of anthracycline cardiomyopathy. Int J Cardiol. 2016;205:99-110.

33. Wang A J, Zhang J, Xiao M, Wang S, Wang B J, Guo Y, et al. Molecular mechanisms of doxorubicin-induced cardiotoxicity: novel roles of sirtuin 1-mediated signaling pathways. Cell Mol Life Sci. 2021;78(7):3105-3125.

34. Koga T, Suico MA, Shimasaki S, Watanabe E, Kai Y, Koyama K, et al. Endoplasmic reticulum (ER) stress induces sirtuin 1 (SIRT1) expression via the PI3K-Akt-GSK3β signaling pathway and promotes hepatocellular injury. J Biol Chem. 2015;290(51):30366-30374.

35. Huang D, Yan ML, Chen KK, Sun R, Dong ZF, Wu PL, et al. Cardiac-specific overexpression of silent information regulator 1 protects against heart and kidney deterioration in cardiorenal syndrome via inhibition of endoplasmic reticulum stress. Cell Physiol Biochem. 2018;46(1):9-22. Erratum in: Cell Physiol Biochem. 2020;54(5):1085-1087.

36. Prola A, Pires Da Silva J, Guilbert A, Lecru L, Piquereau J, Ribeiro M, et al. SIRT1 protects the heart from ER stress-induced cell death through eIF2α deacetylation. Cell Death Differ. 2017;24(2):343-356.

37. Han D, Li X, Li S, Su T, Fan L, Fan WS, et al. Reduced silent information regulator 1 signaling exacerbates sepsis-induced myocardial injury and mitigates the protective effect of a liver X receptor agonist. Free Radic Biol Med. 2017;113:291-303.

38. Hsu YJ, Hsu SC, Hsu CP, Chen YH, Chang YL, Sadoshima J, et al. Sirtuin 1 protects the aging heart from contractile dysfunction mediated through the inhibition of endoplasmic reticulum stress-mediated apoptosis in cardiac-specific sirtuin 1 knockout mouse model. Int J Cardiol. 2017;228:543-552.

39. Chen JY, Hu RY, Chou HC. Quercetin-induced cardioprotection against doxorubicin cytotoxicity. J Biomed Sci. 2013;20(1):95.

40. Dong Q, Chen L, Lu Q, Sharma S, Li L, Morimoto S, et al Quercetin attenuates doxorubicin cardiotoxicity by modulating Bmi-1 expression. Br J Pharmacol. 2014;171(19):4440-4454.

41. Zhang YM, Zhang ZY, Wang RX. Protective mechanisms of quercetin against myocardial ischemia reperfusion injury. Front Physiol. 2020;11:956.

42. Syahputra RA, Harahap U, Dalimunthe A, Nasution MP, Satria D. The role of flavonoids as a cardioprotective strategy against doxorubicin-induced cardiotoxicity: a review. Molecules. 2022;27(4):1320.

43. Batiha GE, Beshbishy AM, Ikram M, Mulla ZS, El-Hack MEA, Taha AE, et al. The pharmacological activity, biochemical properties, and pharmacokinetics of the major natural polyphenolic flavonoid: quercetin. Foods. 2020;9(3):374.

44. Bartlett JJ, Trivedi PC, Pulinilkunnil T. Autophagic dysregulation in doxorubicin cardiomyopathy. J Mol Cell Cardiol. 2017;104:1-8.

45. Alkuraishy HM, Al-Gareeb AI, Al-hussaniy HA. Doxorubicin-induced cardiotoxicity: molecular mechanism and protection by conventional drugs and natural products. Int J Clin Oncol Cancer Res. 2017;2(2):31-44.

46. Sharma A, Parikh M, Shah H, Gandhi T. Modulation of Nrf2 by quercetin in doxorubicin-treated rats. Heliyon. 2020;6(4):e03803

47. Alshammari GM, Al-Qahtani WH, AlFaris NA, Albekairi NA, Alqahtani S, Eid R, et al. Quercetin alleviates cadmium chloride-induced renal damage in rats by suppressing endoplasmic reticulum stress through SIRT1-dependent deacetylation of Xbp-1s and eIF2α. Biomed Pharmacother. 2021;141:111862.

48. Cao D, Wang M, Qiu X, Liu D, Jiang H, Yang N, et al. Structural basis for allosteric, substrate-dependent stimulation of SIRT1 activity by resveratrol. Genes Dev. 2015;29(12):1316-1325.

49. Iside C, Scafuro M, Nebbioso A, Altucci L. SIRT1 activation by natural phytochemicals: an overview. Front Pharmacol. 2020;11:1225.

50. Gad ES, Ashour AM, Gad AM, Khames A, Ibrahim SG, Gadelmawla MHA, et al. Hepatoprotection by methylene blue against doxorubicin toxicity through coordinated modulation of oxidative stress, ER stress, and apoptotic pathways. Pharmaceuticals (Basel). 2025;18(11):1625.

51. Radeva L, Yoncheva K. Doxorubicin toxicity and recent approaches to alleviating its adverse effects with focus on oxidative stress. Molecules. 2025;30(15):3311.

52. Arozal W, Eziefule OM, Wanandi SI, Louisa M, Dewi S, Nafrialdi, et al. Doxorubicin-induced nephrotoxicity: the protective role of a standardized ethanolic extract of *Andrographis paniculata* leaves. Front Pharmacol. 2025;16:1585965.

53. Kebieche M, Lakroun Z, Lahouel M, Bouayed J, Meraihi Z, Soulimani R. Evaluation of epirubicin-induced acute oxidative stress toxicity in rat liver cells and mitochondria, and the prevention of toxicity through quercetin administration. Exp Toxicol Pathol. 2009;61(2):161-177.

54. Rahmani F, Najafizadeh P, Mousavi Z, Rastegar T, Barzegar E. The protective effect of quercetin against hepatotoxicity induced by doxorubicin in male rats. Iranian. Iranian J Pharmacol Ther. 2018;16:1-8.

55. Parabathina RK, Swamy PL, Harikrishna VVSN, SrinivasaRao G, Rao KS. Vitamin-E, morin, rutin, quercetin prevents tissue biochemical changes induced by doxorubicin in oxidative stress conditions: effect on heart, liver and kidney homogenates. J Chem Pharm Res. 2010;2(4):826-834.

56. Köroğlu R, Gül SS, Aygün H. Evaluation of preventive effect of quercetin on doxorubicin-induced nephrotoxic rat model by [99m Tc] Tc-DMSA renal cortical scintigraphy and biochemical methods. Iranian Journal of Nuclear Medicine. 2023;31(2):112-118.